ISSN 1674-1056
http://cpb.iphy.ac.cn
http://iopscience.iop.org/cpb
中国物理 B
Chinese Physics
中国物理 Chinese Physics B

# Controllable preparation and disorder-dependent photoluminescence of morphologically different $C_{60}$ microcrystals

Wen Cui(崔雯), De-Jun Li(李德军), Jin-Liang Guo(郭金良), Lang-Huan Zhao(赵琅嬛), Bing-Bing Liu(刘冰冰), and Shi-Shuai Sun(孙士帅)

**Citation:**Chin. Phys. B, 2021, 30 (**8**): 086101. DOI: 10.1088/1674-1056/ac0691
Journal homepage: http://cpb.iphy.ac.cn; http://iopscience.iop.org/cpb

**What follows is a list of articles you may be interested in**

---

## Water and nutrient recovery from urine: A lead up trail using nano-structured $In_2S_3$ photo electrodes

R Jayakrishnan, T R Sreerev, and Adith Varma
Chin. Phys. B, 2021, 30 (**5**): 056103. DOI: 10.1088/1674-1056/abd169

## Characterization of swift heavy ion tracks in $MoS_2$ by transmission electron microscopy

Li-Jun Xu(徐丽君), Peng-Fei Zhai(翟鹏飞)†, Sheng-Xia Zhang(张胜霞), Jian Zeng(曾健), Pei-Pei Hu(胡培培), Zong-Zhen Li(李宗臻), Li Liu(刘丽), You-Mei Sun(孙友梅), and Jie Liu(刘杰)‡
Chin. Phys. B, 2020, 29 (**10**): 106103. DOI: 10.1088/1674-1056/abad1e

## Irradiation hardening behaviors of tungsten-potassium alloy studied by accelerated 3-MeV $W^{2+}$ ions

Xiao-Liang Yang(杨晓亮), Long-Qing Chen(陈龙庆), Wen-Bin Qiu(邱文彬), Yang-Yi-Peng Song(宋阳一鹏), Yi Tang(唐毅), Xu-Dong Cui(崔旭东), Chang-Song Liu(刘长松), Yan Jiang(蒋燕), Tao Zhang(张涛), Jun Tang(唐军)
Chin. Phys. B, 2020, 29 (**4**): 046102. DOI: 10.1088/1674-1056/ab75cf

## Micron-sized diamond particles containing Ge-V and Si-V color centers

Hang-Cheng Zhang(章航程), Cheng-Ke Chen(陈成克), Ying-Shuang Mei(梅盈爽), Xiao Li(李晓), Mei-Yan Jiang(蒋梅燕), Xiao-Jun Hu(胡晓君)
Chin. Phys. B, 2019, 28 (**7**): 076103. DOI: 10.1088/1674-1056/28/7/076103

## Synthesis of Pr-doped ZnO nanoparticles: Their structural, optical, and photocatalytic properties

Jun-Lian Chen(陈军联), Neena Devi, Na Li(李娜), De-Jun Fu(付德君), Xian-Wen Ke(柯贤文)
Chin. Phys. B, 2018, 27 (**8**): 086102. DOI: 10.1088/1674-1056/27/8/086102

---

# Controllable preparation and disorder-dependent photoluminescence of morphologically different $C_{60}$ microcrystals*

Wen Cui(崔雯)[1,†], De-Jun Li(李德军)[1], Jin-Liang Guo(郭金良)[1], Lang-Huan Zhao(赵琅嬛)[1], Bing-Bing Liu(刘冰冰)[2], and Shi-Shuai Sun(孙士帅)[3,‡]

[1] *College of Physics and Materials Science, Tianjin Normal University, Tianjin* 300387, *China*
[2] *State Key Laboratory of Superhard Materials, Jilin University, Changchun* 130012, *China*
[3] *College of Science, Tianjin University of Technology, Tianjin* 300384, *China*

(Received 18 March 2021; revised manuscript received 26 May 2021; accepted manuscript online 29 May 2021)

Different $C_{60}$ crystals were synthesized by precipitation from a mixture of the good solvent m-xylene and the poor solvent isopropyl alcohol. The samples were characterized by scanning electron microscopy (SEM), Raman spectroscopy, thermogravimetric analysis, and high resolution transmission electron microscope (HRTEM). We found that the morphologies and sizes of the samples could be controlled by adjusting the volume ratio between the good and poor solvents. Especially, an unexpected short flower column-like crystal was synthesized at low ratios (from 1:6 to 1:12). Room temperature photoluminescence (PL) and HRTEM studies of the $C_{60}$ crystal samples reveal that the PL efficiency of the crystals decreases with increasing crystalline order and that the disordered $C_{60}$ crystals synthesized at the ratio of 1:2 show 10 times higher PL efficiency than that of pristine $C_{60}$. The mechanism of the growth process of these $C_{60}$ crystals was also studied by replacing the good solvents m-xylene with toluene and mesitylene.

**Keywords:** $C_{60}$ crystals, morphology, photoluminescence, growth process

**PACS:** 61.48.–c, 68.37.Hk, 78.55.–m, 81.10.–h **DOI:** 10.1088/1674-1056/ac0691

## 1. Introduction

Molecular carbon, such as fullerene $C_{60}$ continues to attract significant attention due to its unique structures and excellent physical and chemical properties.[1–7] Because fullerene properties depend strongly on crystals size, morphology, and structure, large efforts have been devoted to synthesize $C_{60}$ crystals with different morphologies and structures. For example, $C_{60}$ nanorods produced by a slow evaporation method exhibited highly enhanced photoluminescence (PL)[8,9] and disk-type $C_{60}$ structures synthesized by a vapor–solid process can be used in optical devices due to their photoconductivity[10] Miyazawa *et al.* used a liquid–liquid interfacial precipitation (LLIP) method to produce $C_{60}$ nanowhiskers and nanotubes, which can be used in nanoelectronics due to their excellent electronic property.[11,12] Solution-phase crystallization methods are useful to synthesize different types of $C_{60}$ crystals because the crystallization environment can be controlled by adjusting various parameters. However, due to the many parameters involved, the formation mechanism of $C_{60}$ crystals with different morphologies and designed sizes is still elusive and there is a need for further systematic studies.

In the precipitation method, fullerenes spontaneously aggregate in two-solvent mixtures of good and poor solvents for fullerenes, and the resulting geometrical and morphological structures are determined by the type and molecular shape of the solvents. For example, $C_{60}$ wires were synthesized from m-xylene while $C_{60}$ disks were formed when this solvent was replaced by $CCl_4$.[13] Furthermore, the shapes of $C_{60}$ and $C_{70}$ crystals changed by using various aromatic solvents.[14–16] It should be noted that the initial crystals formed usually contain significant amounts of solvent, but this can usually be removed from the solvates (co-crystals) by careful heat treatment without changing the crystal morphology (However, the lattice structure often changes). Other options such as changing the volume ratio between good and poor solvents can also be used to adjust the crystallization environment. For example, rod-shaped $C_{60}$ can be transformed to tube-shaped crystals by changing the volume ratio between m-xylene and isopropyl alcohol (IPA) with different volume ratios.[17] Also, cube- and tube-shaped $C_{70}$ crystals were obtained selectively by reprecipitation using a combination of mesitylene and IPA with different volume ratios.[18] Thus, the mixing ratio of good solvent to poor solvent plays an important role for the cocrystallization of fullerene and solvent. However, the effect of the mixing ratio on the formation process of cocrystals is different for different solvents. A detailed study of the growth mechanism of different $C_{60}$ crystals under various growth conditions

*Project supported by the National Natural Science Foundation of China (Grant Nos. 11504269 and 11504267), Tianjin Natural Science Foundation (Grant No. 20JCQNJC00660), and the Program for Innovative Research in University of Tianjin (Grant No. TD13-5077).

†Corresponding author. E-mail: cuiwen2005xj@126.com
‡Corresponding author. E-mail: sssdashuai@163.com

 

by changing the mixing ratio for different solvents is a challenging project.

To further increase the understanding of how the structure, size, and morphology can be controlled in order to tune the properties of $C_{60}$ crystals for potential applications we have made a systematic study of $C_{60}$ crystal synthesis by precipitation from a mixture of the good solvent m-xylene and the poor solvent IPA. We focused on the effect of varying the precipitation conditions, such as different combinations of solvents and different volume ratios between good and poor solvents. By simply tuning this ratio rod-like, tube-like or short flower column-like crystals could be synthesized. PL measurements on the $C_{60}$ crystals show that the volume ration of the solvents also significantly influences the PL properties.

## 2. Experiment

Excess $C_{60}$ powder (The $C_{60}$ powder with the purity of 99.99% was purchased from XFNANO of Nanjing and the powder was used directly in our experiment without treatment) was dissolved in m-xylene without any treatment for 24 h to form saturated $C_{60}$/m-xylene solution. Known amounts of this $C_{60}$/m-xylene solution were added into different proportions of IPA (the volume ratio of $C_{60}$/m-xylene to IPA was varied from 1:1 to 1:12). The mixture was briefly ultrasonicated for the first 30 s after rapid addition and then kept at room temperature without any further agitation for 24 h. Finally, a black precipitate was found on the bottom of the container. For comparison, toluene and mesitylene were also used as good solvents to synthesize $C_{60}$ crystals. The crystals were characterized by scanning electron microscopy (SEM) on a SU8010, by Raman spectroscopy (HORIBA Jobin Yvon XploRA PLUS), and by high resolution transmission electron microscopy (HRTEM) on a JEM-2010, Japan at an accelerating voltage of 200 kV. All measurements were carried out at room temperature. The PL spectra were recorded using an Ar+ laser (532 nm) at low power (2.6 mW) under ambient conditions. Thermogravimetric analysis (TGA) was carried out under an argon atmosphere and the crystals were heated from room temperature to 1000 °C with a rate of increase of 10 °C/min.

## 3. Results and discussion

Figure 1 shows typical SEM images of the as-grown $C_{60}$ rod-shape crystals synthesized using different volume ratios of $C_{60}$/m-xylene and IPA. From this figure, we can see that similar rod-shaped crystals with hexagonal cross sections were obtained with mixing ratios ranging from 1:1 to 1:4 while the average length of the $C_{60}$ rods gradually decreased from 3 μm–5 μm to 0.6 μm–1 μm as the amount of IPA increased. A similar phenomenon was also found in $C_{70}$/mesitylene, for which it was reported that the average size of the $C_{70}$ cubes decreased when reducing the mixing ratio of good and poor solvents.[15] This result can be explained by the hypothesis that the addition of IPA induces local growth units (droplets) of m-xylene in which $C_{60}$ molecules are localized before crystallization starts. Since the size of the unit became smaller as the amount of IPA was increased and long-range diffusion of $C_{60}$ was unlikely, the average size of the resulting crystal was also smaller. Even more interesting, by further reducing the mixing ratio (from 1:6 to 1:12), short flower column-like crystals were obtained. We also found that the proportion of this "new" type of crystal increased and that the average length slightly changed from 0.8 μm to 0.4 μm with the increasing proportions of IPA (note that the width was changed slightly under all studied conditions, the average size was 400 nm–600 nm). To further investigate the entrapment of solvent molecules in the crystals, a TGA measurement was carried out under argon atmosphere. The result is shown in Fig. 2, where we chose the composition of 1:1 as an example. The crystals started to lose weight around 50 °C and the weight decreased by 5% as the temperature was increased to 193 °C. This weight loss was assumed to be caused by the release of the solvents trapped in the crystals.[17,19] The main weight loss (80%) started at around 600 °C and was due to the sublimation of $C_{60}$. These changes indicated that the composition molar ratio of $C_{60}$ to m-xylene is about 2.4:1, which indicated that the crystals obtained were indeed solvates and that relative amount of m-xylene should be the key factor for the determining the morphology.

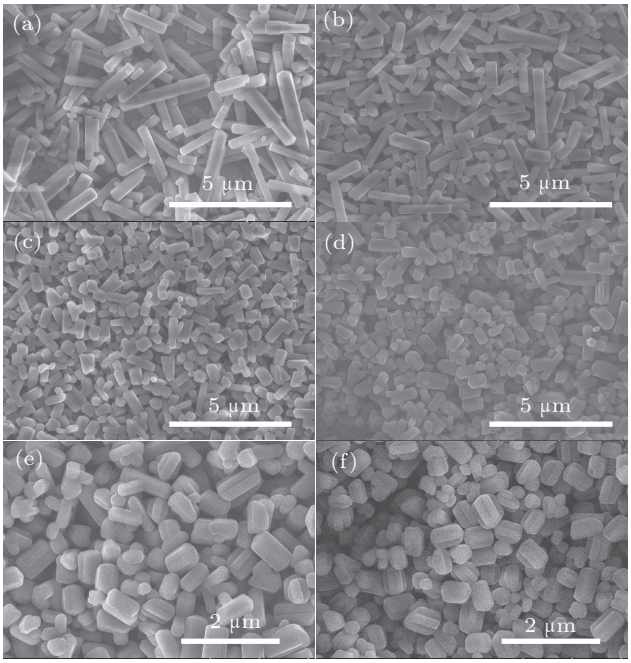


**Fig. 1.** The SEM images of the samples synthesized using different volume ratios of $C_{60}$/m-xylene and IPA: (a) 1:1; (b) 1:2; (c) 1:4; (d) 1:6; (e) 1:8; (f) 1:12.

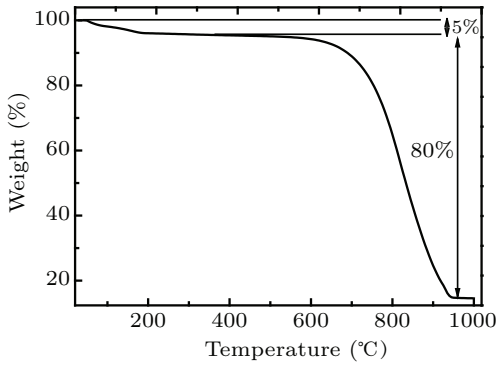


**Fig. 2.** TGA analysis of $C_{60}$/m-xylene under argon atmosphere.

Our results were very different from those of Ji *et al.*,[17] who found that the morphologies of the synthesized crystals varied from rod and tube shape to fence- or palisade-like shapes when the volume ratio of $C_{60}$/m-xylene to IPA decreased. From many previous studies,[20–22] we know that when a solution of fullerenes in good solvent is injected rapidly into a poor solvent, small emulsion droplets of the good solvent are formed immediately. The contact of fullerene molecules with the poor solvent is energetically unfavorable and they prefer to stay surrounded by good solvent molecules. When the concentration of fullerene inside the droplets reaches the saturation point, the crystallization process quickly takes place and fullerene crystals are formed. During the crystal growth after nucleation, due to the concentration depletion effect, the $C_{60}$ molecules prefer to occupy the corners of the hexagonal cross section because of the relatively higher free energy in corner sites. The next most preferred sites are the edges of the hexagonal cross section and the least preferred is the central portion of the hexagonal cross section. Thus with increasing amount of IPA, the concentration depletion effect becomes more severe which leads to the formation of tube and fence-like crystals in the study of Ji *et al*. However, no tube structure was observed in our study even when the mixing ratio was decreased to 1:12. We believe that the different concentrations of $C_{60}$ in m-xylene lead to the key difference between Ji's work and ours. In their work the concentrations of $C_{60}$ in m-xylene ranged from 0.75 mg/mL to 1.5 mg/mL, which was far from the saturation point (approximately 4.8 mg/ml in this work which is similar with the previous report[23]). Thus when more IPA was added, the concentration of $C_{60}$ in the solution became much lower, leading to the formation of tube and fence-like crystals as described above. However, because a saturated solution of $C_{60}$/m-xylene was used here, the high concentration of $C_{60}$ compensates the concentration depletion effect in the central portion of the growing faces, leading to the formation of rodlike structures even at the lowest volume ratio of 1:12.

The observation of short flower column-like crystals was a surprise. We suggested that this unusual shape was formed under highly supersaturated conditions when a large amount of IPA was added. Earlier work showed that the supersaturation ratio influenced the relative growth rate of different facets when crystallization occurred under supersaturated conditions, and it was therefore widely considered to be a determining factor for the final morphology of organic/inorganic crystals.[24–26] This dependence of crystal morphology on the supersaturation ratio was also observed in $C_{60}$ crystallization.[27] Thus it was reasonable to speculate that when $C_{60}$ molecules were surrounded by large amounts of IPA the IPA molecules attached to selected growth facets which restricted the growth of these. The growth rate of other facets thus became relatively higher than that of the restricted facets. As we know, the more rapid the growth rate, the quicker the disappearance of the plane. Eventually, the short flower column-like crystals synthesized under appropriate conditions. When the ratio of $C_{60}$/m-xylene to IPA increased (*i.e.*, the relative amount of IPA is small), $C_{60}$ molecules could occupy the concave angle for continuous growth and the amount of short flower column shape is gradually decreased. This growth mechanism was sketched in Fig. 3

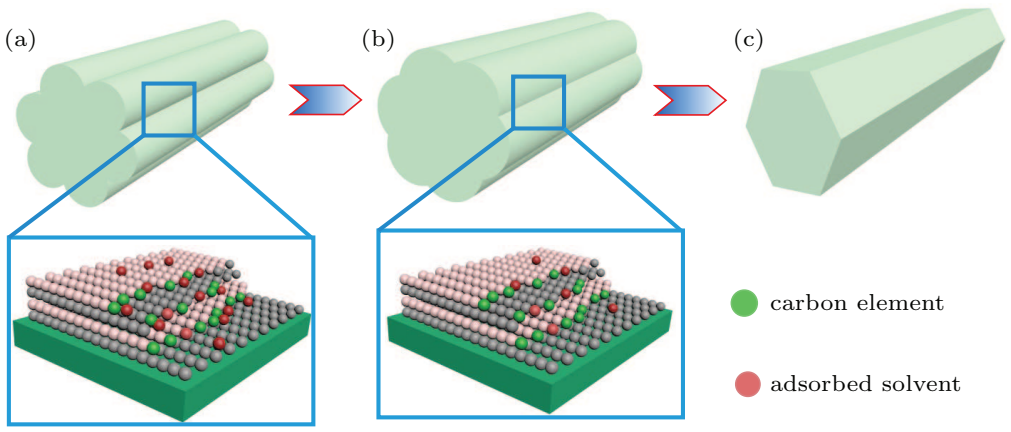


**Fig. 3.** Possible scheme of the growth mechanism of $C_{60}$/m-xylene crystals under different mixing conditions.

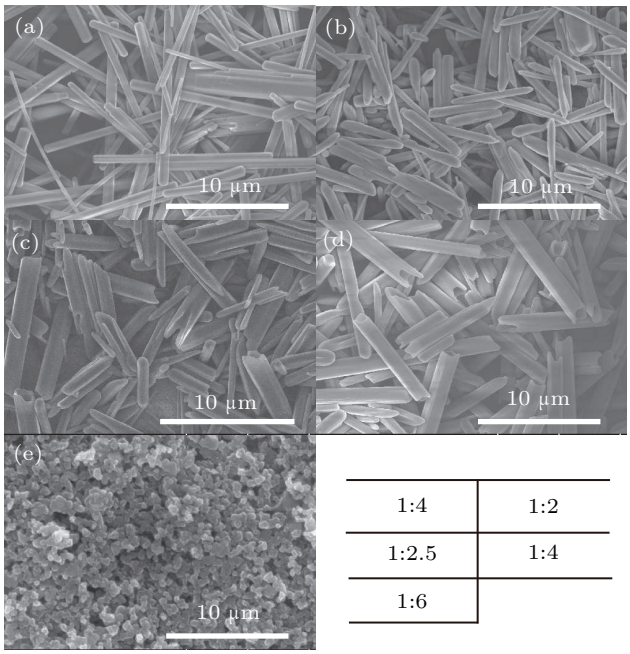


**Fig. 4.** SEM images of $C_{60}$/mesitylene crystals obtained using different volume ratios between $C_{60}$/mesitylene and IPA: (a) 1:1; (b) 1:2; (c) 1:2.5; (d) 1:4; (e) 1:6.

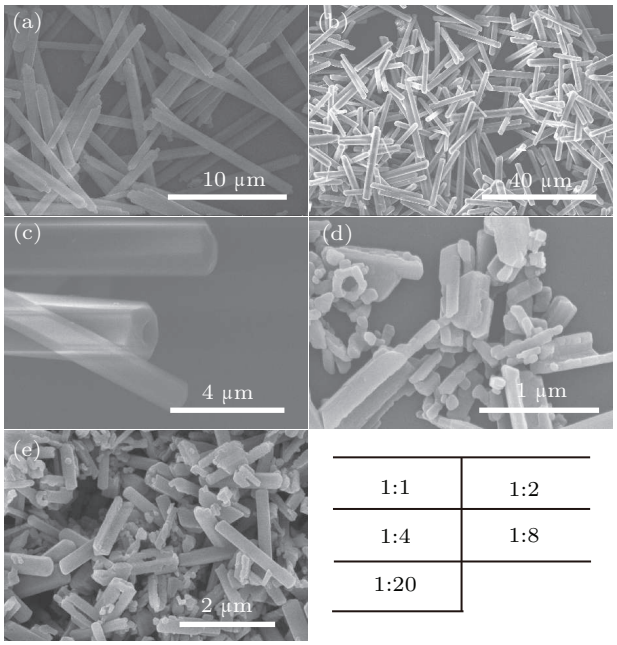


**Fig. 5.** SEM images of $C_{60}$/toluene crystals obtained using different volume ratios between $C_{60}$/toluene and IPA: (a) 1:1; (b) 1:2; (c) 1:4; (d) 1:8; (e) 1:20.

To further clarify the effect of different good solvents and different mixing ratios of solvated $C_{60}$ to IPA on the morphology of the synthesized products, we tried using toluene and mesitylene instead of m-xylene. Figures 4 and 5 show the SEM images of $C_{60}$/mesitylene and $C_{60}$/toluene crystals, respectively, obtained using different volume ratios. We can see that the 1D (linear) $C_{60}$/solvent crystals were also obtained under all conditions studied. For $C_{60}$/mesitylene, rod-like crystals were synthesized at the mixing ratios of 1:1 and 1:2 but for ratios 1:2.5 and higher tube-like shape crystals were obtained. However, at the ratio of 1:6 only $C_{60}$ particles can be observed, indicating mesitylene cannot control the growth of $C_{60}$ molecules under this condition. On the other hand, in $C_{60}$/toluene the morphologies also changed from rod-like shape to tube-like (or hollow) when the mixing ratio changed from 1:1 to 1:12. The difference was that the tube-like shaped crystals formed from the ratio of 1:4 (much lower than for $C_{60}$/mesitylene). However, no tube-like crystals were observed under any conditions from $C_{60}$/m-xylene. On the basis of these experimental findings, a schematic illustration of the formation pathway of $C_{60}$ 1D submicrometer structures in three $C_{60}$ systems with different volume ratios was proposed in Fig. 6.

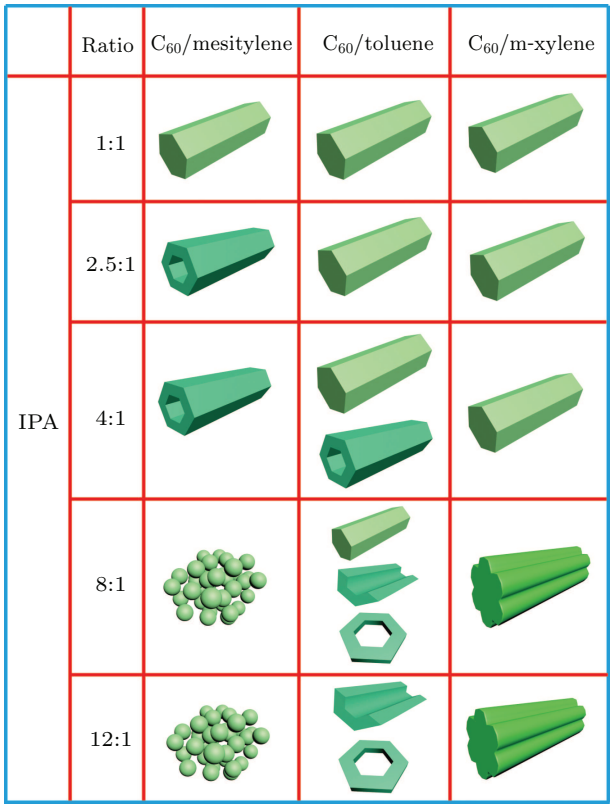


**Fig. 6.** Schematic illustration of the formation pathway of 1D submicrometer $C_{60}$ structures in three systems with different volume ratios.

We have demonstrated that the different solubilities of $C_{60}$ in the solvents is the reason for the different crystal morphologies obtained in these systems. Because the lowest solubility of $C_{60}$ is found for mesitylene (about 1.5 mg/ml), the concentration of $C_{60}$ reaches the saturation point already when a small amount of IPA was added, and $C_{60}$ seeds were immediately formed and started to grow. Due to the concentration depletion effect, the $C_{60}$ molecules prefer to attach to growing sites at corners and edges but not to the central portions of the growing faces of each seed.[17] This resulted in the formation of hexagonal tubes. Due to the small quantity of $C_{60}$ molecules in each local growth unit caused by the low initial concentration of $C_{60}$ in mesitylene compared to the other two solutions, only few $C_{60}$ molecules were available for the further growth

of the crystal and the tube-like shape was maintained even after a long reaction time. For $C_{60}$/toluene, the solubility of $C_{60}$ (2.8 mg/ml) is higher than that in mesitylene and thus adding an additional amount of IPA could induce the formation of tube-like or hollow crystals. Finally, due to the high solubility of $C_{60}$ in m-xylene the concentration depletion effect in the central portion of the growing faces was negligible under all conditions studied which explained why no tube-like crystals were observed even at the mixing ratio of 1:12.

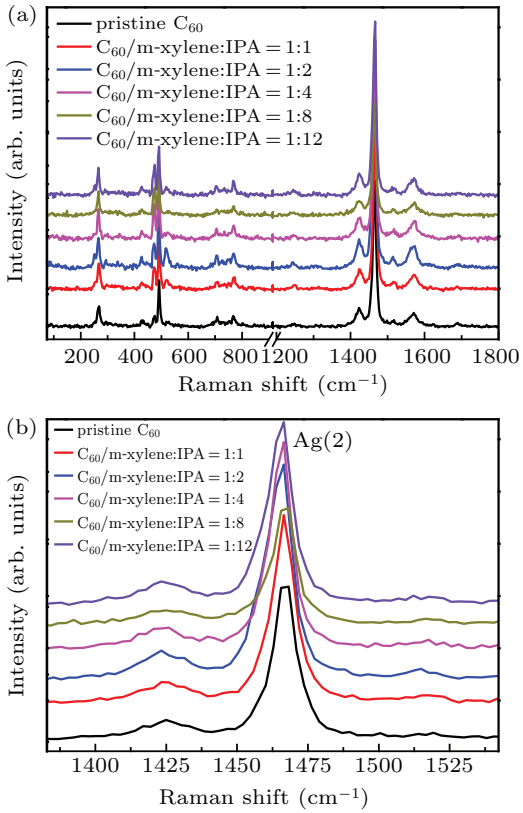


**Fig. 7.** Raman spectra of $C_{60}$/m-xylene rod crystals synthesized under different conditions.

In order to further study the effect of IPA solvent additions on the structure and properties of $C_{60}$/m-xylene, Raman spectroscopy was employed as a powerful tool to characterize $C_{60}$ and $C_{60}$-based materials. The Raman spectra of $C_{60}$/m-xylene rod crystals synthesized under different conditions are shown in Fig. 7. The spectrum of pristine $C_{60}$ was also recorded for comparison. For $C_{60}$ bulk materials, there are 10 vibration bands, *i.e.*, two Ag [Ag(1) and Ag(2)] modes and six Hg [Hg(1), Hg(2), Hg(3), Hg(4), Hg(5), Hg(6), Hg(7), and Hg(8)] modes. From Fig. 7, we can see that all these Raman active bands were observed both in pristine $C_{60}$ and in $C_{60}$/m-xylene crystals. We know that the Ag(2) mode is the characteristic peak of $C_{60}$ and the shift of this band toward lower frequency is an indication of polymerization of $C_{60}$ molecules. We noted that the Ag(1), Ag(2), and Hg(1)–Hg(8) modes of $C_{60}$ molecules were almost unchanged in the rod-like crystals, demonstrating that no polymerization takes place during the synthesis process and that the $C_{60}$/m-xylene crystals consisted of monomeric $C_{60}$. We also found that some new weak peaks appear in the lower frequency range 300 $cm^{-1}$–600 $cm^{-1}$ for $C_{60}$/m-xylene crystals. These peaks were not found in spectra from pure $C_{60}$ or m-xylene. Similar phenomena were also found in $C_{60}$/m-xylene solutions (without IPA solvent) and some other $C_{60}$ solvent materials, and were thus attributed to the interaction between $C_{60}$ and m-xylene molecules.[28] For comparison, we also changed the poor solvent IPA to methanol and ethanol to repeat the above experiment for synthesizing $C_{60}$ crystals. We found that with the increase of alcohols solvents, the morphology changing process of the obtained products is similar with the system of $C_{60}$/m-xylene-IPA, *i.e.*, the length of the products became shorter. However, the crystallinity in $C_{60}$/m-xylene-methanol and $C_{60}$/m-xylene-ethanol is lower than that in $C_{60}$/m-xylene-IPA.

Owing to the excellent photo carrier generation efficiency of $C_{60}$ molecules, the PL of $C_{60}$ crystals can be used to study their optical properties for potential applications as photoreceptors or in photovoltaic systems.[29,30] The PL spectra of the $C_{60}$/m-xylene-IPA system and of pristine $C_{60}$ are shown in Fig. 8. From this figure, we found that the PL energies typically range from 1.6 eV to 1.8 eV for all samples, which was in good agreement with previous reports.[8,31] For all the $C_{60}$/m-xylene crystals the intensity of the PL was significantly enhanced compared to that for pristine $C_{60}$ and the intensity increases when the mixing ratio decreased to 1:2. However, with the ratio decreased further the strength of the PL was also decreased. As extensively reported for pure fullerenes $C_{60}$ and $C_{70}$, PL is enhanced relative to that of the fullerene powder upon formation of microstructures, owing to the improved crystallinity.[10,15,32] To find out if the enhanced PL in our study was also induced by the high crystallinity of the crystal, an HRTEM analysis was carried out. Images of samples synthesized with different mixing ratios of $C_{60}$/m-xylene and IPA are shown in Fig. 9. From this analysis, we found that with decreasing mixing ratio, the degree of structural order was surprisingly increased (except for the 1:1 composition). If we look at the PL spectra and the TEM images, it seemed that the PL intensity increased with increasing disorder. A similar phenomenon was also observed in a recent publication on $Tb_3N@C_{80}$.[33] As we know, pure fullerenes in general have a very low PL intensity because optical excitations to the first excited singlet state very quickly transfer to a long-lived triplet state. PL occurs when a transition from the excited (singlet) state to the (singlet) ground state occurs, but transitions from the triplet excited state to the ground state are forbidden. However, if there are defects, side groups, or solvates, this might interact with the electronic states such that the singlet state is more common and the molecule instead shows a strong PL. Although the detailed PL enhancement mechanism is yet unclear, a plausible interpretation is that increas-

ing disorder could mean increasingly broken symmetry at the molecular level and this could give rise to an increased population of the singlet state, which thus contributes to a strong PL in the 1:2 composition. Interestingly, such an anomalous PL enhancement effect is also observed in $C_{60}$/mesitylene and $C_{60}$/toluene, suggesting that it originates from the microstructure of the crystals and is independent of the nature of the intercalant molecules.

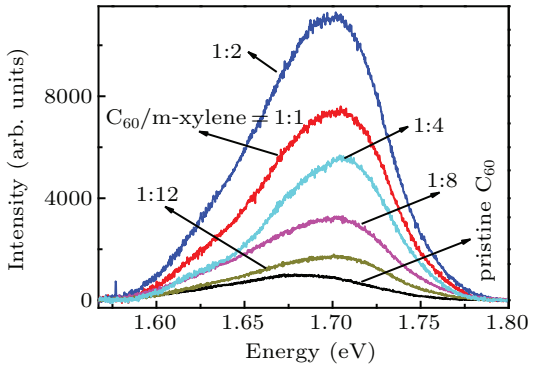


**Fig. 8.** PL spectra of $C_{60}$/m-xylene rod crystals synthesized under different conditions.

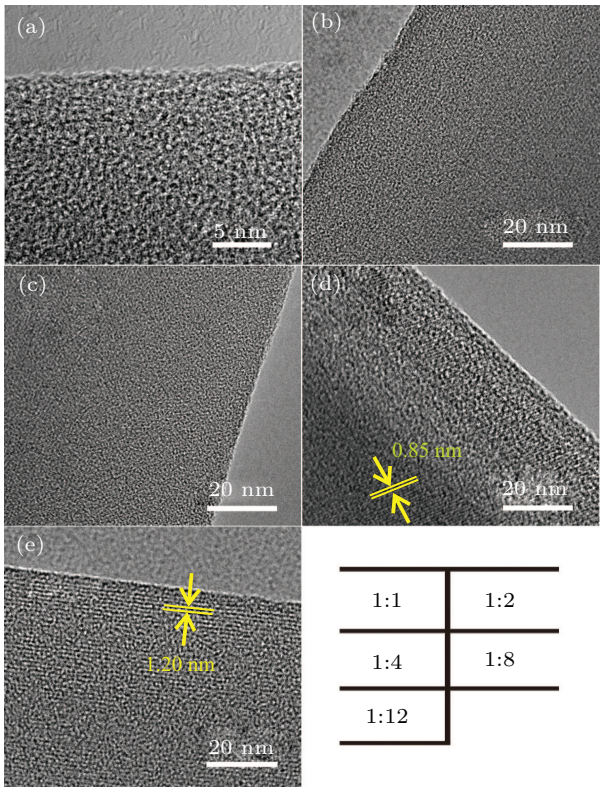


**Fig. 9.** HRTEM images of $C_{60}$/m-xylene crystals obtained from different volume ratios between $C_{60}$/toluene and IPA: (a) 1:1; (b) 1:2; (c) 1:4; (d) 1:8; (e) 1:12.

In addition to the difference in the PL intensity, we also observed a slight blue shift in the PL spectrum of all $C_{60}$ crystals prepared here compared to that of pristine $C_{60}$. A similar blue shift has also been observed in some $C_{60}$ materials, such as $C_{60}$ nanowhiskers, $C_{60}$ nanotubes,[34] and also in 1D organic crystals.[35] HOMO–LUMO (highest occupied molecular orbital–lowest unoccupied molecular orbital) transitions in molecular semiconductors are very sensitive to the distance between nearest molecules so that we anticipate that the blue shift in the PL spectra of the $C_{60}$ microcrystals is due to structural differences in solvated crystals.[36] For example, solvated $C_{60}$ crystals should have a slightly expanded lattice which implies an increased band gap[37] and thus a blue-shifted PL. Another possibility could be the quantum confinement effects in the 1D nanostructures of $C_{60}$ microcrystals which can reduce the symmetry of $C_{60}$, leading to the shift in the PL spectra. A detailed study is still needed to uncover the relation between the structure and the optical properties of the $C_{60}$ microcrystals. Nevertheless, such morphology-dependent optical properties may provide a novel approach to the strategic design of novel optoelectronic functions based on fullerene nanostructures.

## 4. Conclusion

$C_{60}$ crystals with different morphologies were synthesized by precipitation from a mixture of m-xylene and isopropyl alcohol. Through simply adjusting the volume ratio between the good and poor solvents (from 1:1 to 1:12), rod-like and flower column-like crystals were obtained. Comparing with similar experiments and previous work, we found that the solubility of $C_{60}$ in solvents played an important role for the formation of various morphologies. Also, the PL efficiency of $C_{60}$ crystals decreases with crystalline order and reached values 10 times higher than that of pristine $C_{60}$ in the 1:2 composition. It was found that increasing disorder could mean increasingly broken symmetry at the molecular level and give rise to an increased population of the singlet state, which thus contributed to a strong PL in the 1:2 composition.

## References

[1] Komatsu K, Murata M and Murata Y 2005 *Science* **307** 238
[2] Dresselhaus M S, Dresselhaus G and Eklund P C 1997 *Carbon* **35** 437
[3] Minato J and Miyazawa K 2005 *Carbon* **43** 2837
[4] Yao M G, Andersson B M, Stenmark P, Sundqvist B, Liu B B and Wagberg T 2009 *Carbon* **47** 1181
[5] Bae E, Kim N D, Kwak B K, Park J, Lee J, Kim Y, Choi K and Yi J 2010 *Carbon* **48** 3676
[6] Ai M, Li J, Ji Z J, Wang C H, Li R, Dai W and Chen M 2019 *RSC Adv.* **9** 3050
[7] Liu H B, Li Y L, Jiang L, Luo H Y, Xiao S Q, Fang H J, Li H M, Zhu D B, Yu A P, Xu J and Xiang B 2002 *J. Am. Chem. Soc.* **124** 13370
[8] Wang L, Liu B B, Yu S D, Yao M G, Liu D D, Hou Y Y, Tian C, Zou G T, Sundqvist B, You H, Zhang D K and Ma D G 2006 *Chem. Mater.* **18** 4190
[9] Ji H X, Hu J S, Wan L J, Tang Q X and Hu W P 2008 *J. Mater. Chem.* **18** 328
[10] Shin H S, Yoon S M, Tang Q, Chon B, Joo T and Choi H G 2008 *Angew. Chem.* **120** 705
[11] Miyazawa K and Hamamoto K 2002 *J. Mater. Res.* **17** 2205
[12] Xu M, Pathak Y, Fujita D, Ringor C and Miyazawa K 2008 *Nanotechnology* **19** 075712
[13] Park C, Song H J and Choi H C 2009 *Chem. Commun.* 4803
[14] Sathish M and Miyazawa K 2007 *J. Am. Chem. Soc.* **129** 13816
[15] Park C, Yoon E, Kawano M, Joo T and Choi H C 2010 *Angew. Chem., Int. Ed.* **49** 9670

[16] Yao M G, Fan X H, Liu D D, Liu B B and Wagberg T 2012 *Carbon* **50** 209
[17] Ji H X, Hu J S, Tang Q X, Song W G, Wang C R, Hu W P, Wan L J and Lee S T 2007 *J. Phys. Chem. C* **111** 10498
[18] Kim J, Park C and Choi H C 2015 *Chem. Mater.* **27** 2408
[19] Geng J, Zhou W, Skelton P, Yue W, Kinloch I A, Windle A H and Johnson B F G 2008 *J. Am. Chem. Soc.* **130** 2527
[20] Alargova R G, Deguchi S and Tsujii K 2001 *J. Am. Chem. Soc.* **123** 10460
[21] Sun Y P and Bunker C E 1993 *Nature* **365** 398
[22] Bokare A D and Patnaik A 2005 *J. Phys. Chem. B* **109** 87
[23] Ruoff R S, Tse D S, Malhotra R and Lorents D C 1993 *J. Phys. Chem.* **97** 3379
[24] Ouyang J, Pei J, Kuang Q, Xie Z and Zheng L 2014 *ACS Appl. Mater. Interfaces* **6** 12505
[25] Nichols P L, Sun M and Ning C 2011 *ACS Nano* **5** 8730
[26] Zhang X J, Zhao C P, Lv J Y, Dong C, Ou X M, Zhang X H and Lee S T 2011 *Cryst. Growth Des.* **11** 3677
[27] Jeong J, Kim W S, Park S I, Yoon T S and Chung B H 2010 *J. Phys. Chem. C* **114** 12976
[28] Talyzin A and Jansson U 2000 *J. Phys. Chem. B* **104** 5064
[29] Li Y J, Lin Y, Wang N, Li Y L, Liu H B, Lu F S, Zhuang J P and Zhu D B 2005 *Carbon* **43** 1968
[30] Xiao J C, Liu Y, Li Y J, Ye J P, Li Y L, Xu X H, Li X F, Liu H B, Huang C S, Cui S and Zhu D B 2006 *Carbon* **44** 2785
[31] Liu D D, Yao M G, Li Q J, Cui W, Wang L, Li Z P, Liu B, Lv H, Zou B, Cui T, Liu B B and Sundqvist B 2012 *J. Raman Spectrosc.* **43** 737
[32] Jin Y, Curry R J, Sloan J, Hatton R A, Chong L C, Blanchard N, Stolojan V, Kroto H W and Silva S R 2006 *J. Mater. Chem.* **16** 3715
[33] Wu J H, Zhu X J, Guan Y, Wang Y J, Jin F, Guan R N, Liu F P, Chen M Q, Tian Y C and Yang S F 2019 *Angew. Chem. Int. Ed.* **58** 11350
[34] Cha S I, Miyazawa K, Kim Y K, Lee D Y and Kim J D 2011 *J. Nanosci. Nanotechnol.* **11** 3374
[35] Zhang X J, Zhang X H, Zou K, Lee C S and Lee S T 2007 *J. Am. Chem. Soc.* **129** 3527
[36] Shrestha L K, Hill J P, Tsuruoka T, Miyazawa K and Ariga K 2013 *Langmuir* **29** 7195
[37] Meletov K P, Dolganov V K, Zharikov O V, Kremenskaya I N and Ossipyan Y A 1992 *J. Phys. I* **2** 2097